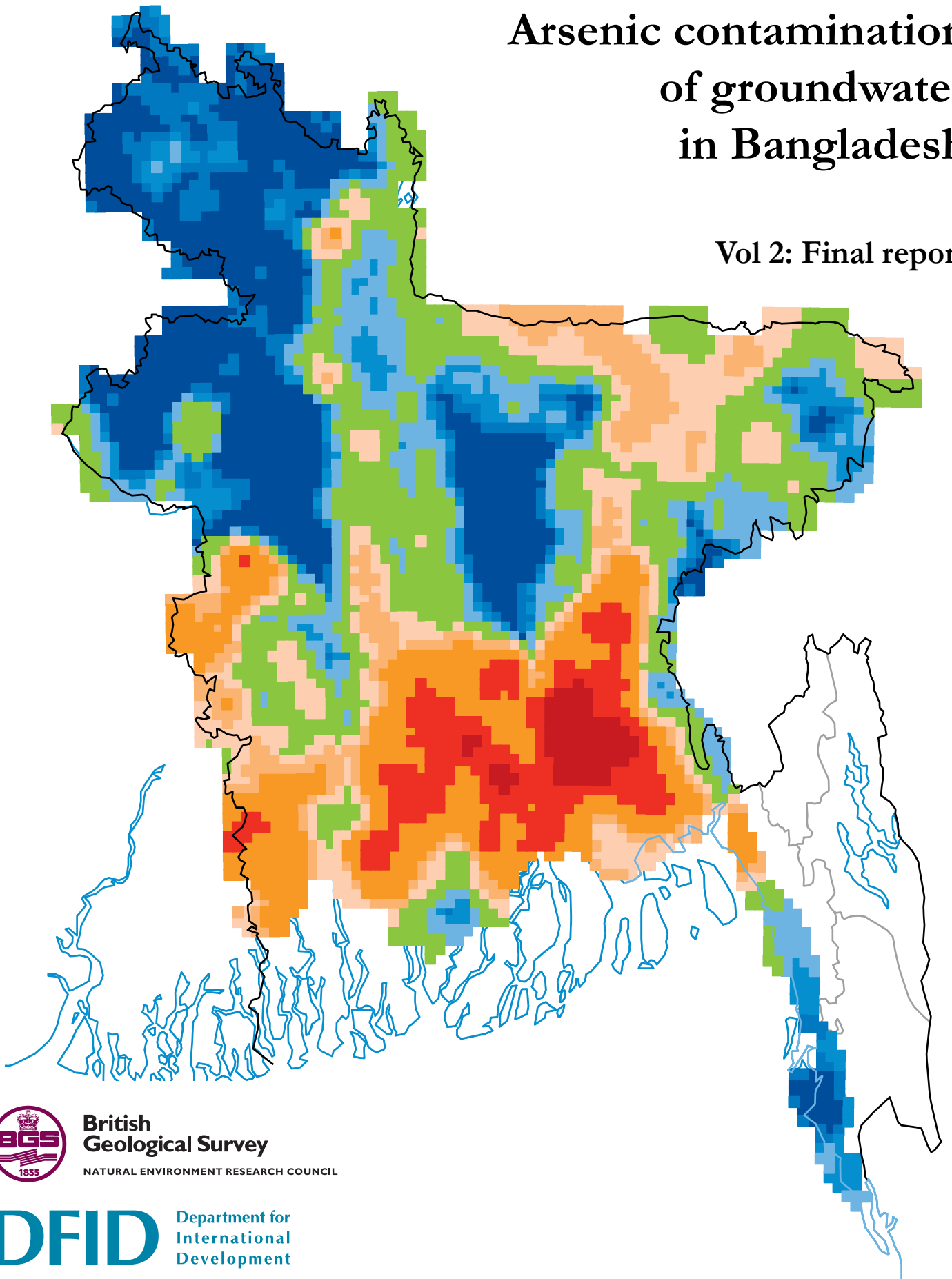


Arsenic contamination of groundwater in Bangladesh

Vol 2: Final report



**British
Geological Survey**

NATURAL ENVIRONMENT RESEARCH COUNCIL

DFID

Department for
International
Development



Government of the People's Republic of Bangladesh
Ministry of Local Government, Rural Development and Co-operatives
Department of Public Health Engineering

Government of the People's Republic of Bangladesh
Ministry of Local Government, Rural Development and Co-operatives
Department of Public Health Engineering

Department for International Development (UK)

British Geological Survey

BGS Technical Report WC/00/19, Volume 2

Arsenic contamination of groundwater in Bangladesh

Vol 2: Final Report

D G Kinniburgh and P L Smedley (Editors)

February 2001

The full report comprises four volumes:

- Volume 1. Summary
- Volume 2. Final report
- Volume 3. Hydrochemical atlas
- Volume 4. Data compilation

Further information can also be viewed and downloaded from our website at www.bgs.ac.uk/arsenic/Bangladesh

This document is an output from a project funded by the UK Department for International Development (DFID). The views expressed are not necessarily those of DFID.

Reproduction of materials contained in this report is granted subject to the inclusion of the following acknowledgement:- “This report was produced by the British Geological Survey and the Department of Public Health Engineering (Bangladesh) undertaking a project funded by the UK Department for International Development (DFID). Any views expressed are not necessarily those of DFID”. In cases where only a map or diagram is reproduced or where data from the report are used, the above acknowledgement may be substituted by a full citation to the report.

Cover Illustration

Map of Bangladesh showing the regional distribution of arsenic in groundwater found during the National Hydrochemical Survey

Bibliographic Reference

BGS AND DPHE, 2001
Arsenic contamination of groundwater in Bangladesh
KINNIBURGH, D G and SMEDLEY, P L (Editors)
Volume 2: Final report
British Geological Survey Report WC/00/19
British Geological Survey, Keyworth.

ISBN 0 85272 384 9

Contributors

Project Director

Kazi Nasiruddin Ahmad, DPHE

Executive Engineer, R&D Division, DPHE

S M Ihtishamul Huq, DPHE

Project Leader

David Kinniburgh, BGS

Deputy Project Leader

Pauline Smedley, BGS

Report Editors

David Kinniburgh and Pauline Smedley, BGS

Database Manager and Report Production Editor

Chris Milne, BGS

Consultant

Kazi Matin Ahmed, DU

Principal Authors

Chapter 1. Introduction

David Kinniburgh, S M Ihtishamul Huq

Chapter 2. Arsenic in groundwaters across the world

Pauline Smedley, David Kinniburgh

Chapter 3. Geology and sedimentology

Jeff Davies

Chapter 4. Hydrogeology

John Chilton, Jeff Davies, Andrew Hughes, Kazi Matin Ahmed, S M Ihtishamul Huq

Chapter 5. Groundwater flow modelling

Andrew Hughes, Emily Whitehead, John Chilton, Jeff Davies

Chapter 6. The National Hydrochemical Survey

David Kinniburgh, Pauline Smedley, Janice Trafford, Chris Milne, S M Ihtishamul Huq, Kazi Matin Ahmed, Simon Burden

Chapter 7. Hydrogeochemistry of three Special Study Areas

Pauline Smedley, David Kinniburgh, Chris Milne, Janice Trafford, Ihtishamul Huq, Kazi Matin Ahmed

Chapter 8. A village survey: Mandari, Lakshmipur district

David Kinniburgh, Walter Kosmus, S M Ihtishamul Huq, Saifur Rahman

Chapter 9. Scales of variation

Irina Gaus, Richard Webster, David Kinniburgh

Chapter 10. Changes with time: piezometer monitoring

Pauline Smedley, David Kinniburgh, Chris Milne, S M Ihtishamul Huq, Kazi Matin Ahmed

Chapter 11. Mineralogy and sediment chemistry

Jonathan Pearce, David Kinniburgh, Pauline Smedley, Kazi Matin Ahmed, Mizanur Rahman

Chapter 12. Sorption and transport

David Kinniburgh

Chapter 13. Conclusions and Recommendations

David Kinniburgh, Pauline Smedley, S M Ihtishamul Huq, Kazi Matin Ahmed

Author Affiliations

Ahmed, Kazi Matin, Dhaka University

Burden, Simon, BGS, Keyworth

Chilton, John, BGS, Wallingford

Davies, Jeff, BGS, Wallingford

Gaus, Irina, BGS, Wallingford

Hughes, Andrew, BGS, Wallingford

Huq, S M Ihtishamul, DPHE, Dhaka

Kinniburgh, David, BGS, Wallingford

Kosmus, Walter, Karl-Franzens University, Graz

Milne, Chris, BGS, Wallingford

Pearce, Jonathan, BGS, Keyworth

Rahman, Mizanur, BWDB, Dhaka

Rahman, Saifur, DPHE, Dhaka

Smedley, Pauline, BGS, Wallingford

Trafford, Janice, BGS, Wallingford

Webster, Richard, Rothamsted Experimental Station

Whitehead, Emily, BGS, Wallingford

Acknowledgements

- Mike McCarthy, DFID
Making the project possible and being supportive
- Denis Peach, BGS
Supporting in many ways
- Joanne Haslam, BGS
BGS project finances
- Peter Ravenscroft, MML
Leading the local input to Phase I
- Md Mizanur Rahman, BWDB; Alamgir Hossain, BWDB
Drilling cored boreholes, installing piezometers, collecting samples from the BWDB monitoring sites and providing water level data and borehole logs
- District Executive Engineers and staff, DPHE
Assisting with the National Hydrochemical Survey
- DPHE officers, Lakshmipur district office
Assisting with the Mandari village survey
- Ashfiquzzaman Aktar, Khairul Amin, Khairul Bashar, Abdul Malek, Abdul Noor, Md Rabiul Islam, Shahidul Islam, Md Ibrahim Khalil, Md Taibur Rahman and Abdus Salam
Fieldwork for the National Hydrochemical Survey
- Mosharraf Hossain and Shah Alam, DPHE
Regular sampling of piezometers
- Pannalal Chowdhury, Abdus Sattar Mia, Siddique Amin Talukder, Fakhir Uddin and laboratory staff, DPHE
Chemical analysis of water samples during Phase I
- Linda Ault, Sally Bourliakas, Simon Burden, Jenny Cook, Kerry Dodd, Suzan Gordon, John Thorns and Janice Trafford, BGS
Chemical and mineralogical analyses
- George Darling, BGS
Stable isotope analyses
- Balt Verhagen, University of Witwatersrand
Tritium analyses
- Charlotte Bryant, Margaret Currie and Brian Miller, NERC Radiocarbon Laboratory, East Kilbride and staff of the AMS Laboratory, University of Arizona
Carbon-14 analyses
- Richard Reynolds, USGS
Sediment magnetic susceptibility measurements and photomicrographs
- Mizanur Rahman, BWDB
Providing sediment samples
- Munir Hussein, GSB
Review of Bangladesh sediments
- Azharul Huq, DWASA
Arranging access to Dhaka deep tubewells
- DFID Transport
Providing vehicles and arranging vehicles for hire
- DFID drivers (Mizan, Abdul, Bimol, PK, Akhter, Zamil, Sultan, Mustafa, Jewel and Shah Jahan)
Good driving and patience!
- Chairman and Union Council Officers, Mandari
Providing logistical support during the village survey
- The people of Mandari
Help during the village survey
- Md Golam Rahman, SPARRSO
Providing satellite images
- Bilqis Amin Hoque, formerly ICDDR,B
Discussions and parallel Phase I microbiological and water quality survey
- Aftab Alam Khan, DU
Discussions and sediment samples
- Meindert Keizer, University of Wageningen
Providing the ECOSAT geochemical speciation and mass transport program
- David Parkhurst, USGS
Providing the PHREEQC geochemical speciation and mass transport program
- Vincent Post
Providing a Windows interface for PHREEQC
- Willem van Riemsdijk and Tjisse Hiemstra, University of Wageningen
Discussions about adsorption processes and modelling over many years
- Tony Appelo, Consultant
Discussions about geochemical modelling and contributions to the development of PHREEQC (Version 2)
- Bob Simons
CoPlot scientific plotting software
- John Whitney, USGS
Discussions
- Quazi Quamruzzaman, DCH
Discussions and survey data
- Gill Tyson
Cartographic work
- Jane Kinniburgh
Help with the Mandari survey

Contents

Contributors	i	6.11 Phosphorus	92
Acknowledgements	ii	6.12 Trace elements: ICP-MS data	93
Contents	iii	6.13 BWDB Water-Quality Monitoring Network	93
List of Figures	v	6.14 Detailed chemistry of Dhaka deep tubewells	97
List of Tables	xi	6.15 Comparison of the arsenic results with those from other large data sets	98
Abbreviations	xv	6.16 Microbiological quality	102
Executive summary	xvii	6.17 Summary	102
1 Introduction	1	7 Hydrogeochemistry of three Special Study Areas	105
2 Arsenic in groundwaters across the world	3	7.1 Introduction	105
2.1 Importance of arsenic in drinking water	3	7.2 Local geology and hydrogeology	105
2.2 Sources of arsenic	3	7.3 Sampling and analytical methods	107
2.3 Mineral-water interactions	7	7.4 Regional groundwater chemistry	109
2.4 Groundwater environments showing enhanced arsenic concentrations	11	7.5 Pore water chemistry: Rajarampur (Chapai Nawabganj)	145
3 Geology and sedimentology	17	7.6 Discussion	146
3.1 Physical Setting	17	7.7 Conclusions	147
3.2 Sea-level change and patterns of sedimentation	22	8 A village survey: Mandari, Lakshmipur District	151
3.3 Regional characterisation of sediments	25	8.1 Introduction	151
3.4 Conceptual models	37	8.2 The village	151
3.5 Summary	43	8.3 Sampling and analysis	153
3.6 Conclusions	46	8.4 Well statistics	155
4 Hydrogeology	47	8.5 Water quality	155
4.1 Introduction	47	8.6 Conclusions	160
4.2 Aquifer distribution	47	9 Scales of variation	161
4.3 Rainfall, runoff and recharge	49	9.1 Introduction	161
4.4 Aquifer properties	51	9.2 Country and district level	161
4.5 Groundwater abstraction and tubewells	52	9.3 Local variation	170
4.6 Groundwater levels	53	9.4 Conclusions	172
4.7 Groundwater usage	55	10 Changes with time: groundwater monitoring	175
4.8 Groundwater flow and aquifer flushing	57	10.1 Introduction	175
4.9 Conceptual model of seasonal flow patterns	59	10.2 Sampling and analysis	175
4.10 Summary	60	10.3 Water levels	176
5 Groundwater flow modelling	63	10.4 Arsenic	178
5.1 Objectives of modelling	63	10.5 Sodium and chloride	180
5.2 Generic model	63	10.6 Sulphate	181
5.3 Site specific model: Faridpur	66	10.7 Phosphate	183
5.4 Groundwater flow near to a meandering river	71	10.8 Conclusions	184
5.5 Summary and conclusions	76	11 Mineralogy and sediment chemistry	187
6 The National Hydrochemical Survey	77	11.1 Sediment samples available	187
6.1 Introduction	77	11.2 Samples selected for mineralogical analysis	189
6.2 Earlier water-quality surveys	77	11.3 Methods	189
6.3 Aims of the National Hydrochemical Survey	78	11.4 Mineralogy and whole rock geochemistry	191
6.4 Survey methodology	78	11.5 Nature and origin of the sediments	200
6.5 Site characteristics	80	11.6 Oxalate extractions	204
6.6 Arsenic	81	11.7 Organic carbon content of sediments	210
6.7 Magnesium, calcium, strontium and barium	88	11.8 Summary	210
6.8 Iron and manganese	88	12 Sorption and transport	213
6.9 Sodium, potassium and boron	90	12.1 Evolution of the groundwater arsenic problem in the Bengal Basin	213
6.10 Sulphate	91	12.2 Transport of arsenic in Bangladesh aquifers	217
		12.3 Modelling arsenic sorption by iron oxides	218

12.4 Modelling the development of arsenic-rich groundwaters	224	13.3 Use of dug wells	237
12.5 Transport of arsenic	228	13.4 Use of deep tubewells	237
12.6 Is the Bengal Basin groundwater arsenic problem unique?	230	13.5 In-situ arsenic removal	238
12.7 Summary	230	13.6 Passive sedimentation	238
13 Conclusions and Recommendations	231	13.7 Siting of new wells	240
13.1 Principal findings	231	13.8 Approach adopted in this study	241
13.2 Groundwater testing for arsenic	234	13.9 Some areas of current debate	241
		13.10 Recommendations for future research	253
		References	257

List of Figures

Figure 2.1. Documented cases of arsenic problems in groundwater related to natural contamination.	11	Figure 3.21. Section B: Geological section from Chapai Nawabganj–Aricha–Sylhet.	41
Figure 3.1. Brahmaputra/Ganges/Meghna delta system: environments of sediment deposition and main geomorphic units.	18	Figure 3.22. Section C: Geological section from Meherpur–Dhaka–Feni.	42
Figure 3.2. Brahmaputra/Ganges/Meghna delta system: tectonic elements.	20	Figure 3.23. Section D: Geological section from Meherpur–Manikganj–Chittagong.	43
Figure 3.3. Map showing the locations of the main hydrogeological studies undertaken in Bangladesh.	21	Figure 3.24. Section E: Geological section from Satkhira–Lakshmipur–Feni.	44
Figure 3.4. Sea-level changes during the last interglacial-glacial transition (after Pirazzoli, 1991).	22	Figure 3.25. Possible main river channels at the time of the last interglacial highstand (120 ka BP).	44
Figure 3.5. Hydrogeological cross-section from north to south across Bangladesh.	25	Figure 3.26. Incisional main river channels at the time of the glacial maximum (21 ka BP).	44
Figure 3.6. The drilling rig used for the construction of the DPHE/BGS Lakshmipur test borehole (LPW6).	26	Figure 3.27. Location of gravity sediment flows and the limits of the marine transgression since the last post-glacial maximum.	45
Figure 3.7. Close-up of the drilling rig used for the construction of the DPHE/BGS Lakshmipur test borehole (LPW6).	27	Figure 4.1. Maximum depth of drilling possible without a powered rig (NWMP, 2000).	47
Figure 3.8. Geological cross section through the Chapai Nawabganj Special Study Area.	28	Figure 4.2. Actual recharge across Bangladesh (from DPHE/BGS/MML, 1999).	50
Figure 3.9. Lithological log of the DPHE/BGS test borehole at Chapai Nawabganj (CPW5). The colouring reflects the colour of the sediments.	28	Figure 4.3. Map of the variation in aquifer transmissivity across Bangladesh.	51
Figure 3.10. Photographs of core from the Chapai Nawabganj test borehole (CPW5).	29	Figure 4.4. Examples of hydrographs from selected sites in the main aquifers of Bangladesh.	54
Figure 3.11. Lithological logs of selected boreholes from Chapai Nawabganj and surrounding areas (DW1 and DW2).	30	Figure 4.5. Map indicating the maximum depth to groundwater.	55
Figure 3.12. Geological cross-section through the Faridpur Special Study Area.	31	Figure 4.6. Change since 1982 in total irrigated area in Bangladesh.	56
Figure 3.13. Lithological log of the DPHE/BGS test borehole at Faridpur (FPW6). The colouring reflects the colour of the sediments.	32	Figure 4.7. Distribution of irrigation technologies used in Bangladesh about 1996.	56
Figure 3.14. Photographs of core from the Faridpur test borehole (FPW6).	33	Figure 4.8. Geological cross-section through the Jamuna Channel alluvial deposits showing the four-layer aquifer structure.	57
Figure 3.15. Lithological log of the DPHE/BGS test borehole at Lakshmipur (LPW6). The colouring reflects the colour of the sediments.	35	Figure 4.9. Hydrogeological cross section through the shallow and deep aquifers of the Faridpur area.	59
Figure 3.16. Photographs of core from the Lakshmipur test borehole (LPW6).	36	Figure 4.10. Conceptual model – basic hydrogeological units and main irrigation pumping methods.	60
Figure 3.17. Geological cross-section through the Lakshmipur Special Study Area.	38	Figure 4.11. Conceptual model – water flow patterns and resultant water levels during the dry season and the following wet season	60
Figure 3.18. Hydrogeological cross section of the south-east GBM delta, showing Late Quaternary sediments.	39	Figure 4.12. Conceptual model – water flow patterns and water level change following the end of the monsoon season and during the early dry season.	61
Figure 3.19. Geological cross-section through the Late Quaternary fluvial sediments within the incised Jamuna channel, central GBM system.	39	Figure 5.1. The vertical slice model.	64
Figure 3.20. Section A: Geological section from Panchagarh–Sherpur–Madaripur.	40	Figure 5.2. Results from basecase vertical slice model. (a) groundwater head profile; (b) particle tracks.	65
		Figure 5.3. Layering used in the vertical slice model.	66
		Figure 5.4. Flowlines for the base case model. Flow travels from the left to a discharge point on the right.	68

Figure 5.5. Flowlines from the surface to STWs for the base case when pumping is included.	69	Figure 6.16. Arsenic concentrations plotted against sulphate concentrations in groundwaters from the Jamuna Valley based on data from the NHS.	92
Figure 5.6. Flowlines to a DTW for the basecase model with pumping included.	70	Figure 6.17. Spatial variation of phosphorus in groundwaters from the National Hydrochemical Survey.	92
Figure 5.7. Generic meander model. Contours of head in metres.	72	Figure 6.18. Arsenic concentrations plotted against phosphorus concentrations in groundwaters from the Jamuna Valley based on data from the NHS.	93
Figure 5.8. Variation of velocity through section through river for the generic meander model (PM1).	72	Figure 6.19. Distribution of well depths in the BWDB Water-Quality Monitoring Network survey.	94
Figure 5.9. Groundwater flow velocity around an idealised meandering river (PM1).	73	Figure 6.20. Chloride distribution in groundwaters from the BWDB Water-Quality Monitoring Network survey.	94
Figure 5.10. Reverse particle tracking demonstrating the divergent flow of groundwater inside the meander and convergent flow outside (PM1).	73	Figure 6.21. Fluoride distribution in groundwaters from the BWDB Water-Quality Monitoring Network survey.	95
Figure 5.11. Groundwater flow velocity around an idealised meandering river with gradient in stage (PM2).	73	Figure 6.22. Iodide distribution in groundwaters from the BWDB Water-Quality Monitoring Network survey.	95
Figure 5.12. Conceptual model of Chapai Nawabganj upazila.	74	Figure 6.23. Nickel distribution in groundwaters from the BWDB Water-Quality Monitoring Network survey.	96
Figure 5.13. Groundwater flow velocity in Chapai Nawabganj.	74	Figure 6.24. Uranium distribution observed in groundwaters from the BWDB Water-Quality Monitoring Network survey.	96
Figure 5.14. Sensitivity of groundwater head to changes in parameters.	75	Figure 6.25. Zinc distribution in groundwaters from the BWDB Water-Quality Monitoring Network survey.	96
Figure 5.15. Normalised sensitivity of groundwater head to changes in parameters.	75	Figure 6.26. Results from the DPHE-UNICEF tubewell screening programme.	98
Figure 6.1. Distribution of well sites and year sampled for the DPHE/BGS National Hydrochemical Survey.	80	Figure 6.27. Location of the upazilas selected for comprehensive screening in Phases I and II of the BAMWSP National Emergency Screening Programme (NESP).	99
Figure 6.2. The depth distribution of wells sampled in the National Hydrochemical Survey.	80	Figure 6.28. Relationships between observations of different surveys	102
Figure 6.3. Map of point-source arsenic concentrations observed in groundwaters in the National Hydrochemical Survey.	83	Figure 7.1. Sketch map of Bangladesh showing the major river systems and the locations of the three Special Study Areas.	105
Figure 6.4. Map of smoothed groundwater arsenic concentrations from the National Hydrochemical Survey.	83	Figure 7.2. Maps of the three study areas showing surface geology	105
Figure 6.5. Average concentration of arsenic in wells from each of the six administrative divisions.	84	Figure 7.3. Maps of the three Special Study Areas showing the distribution of Eh.	106
Figure 6.6. Concentration of arsenic plotted against well depth for all sampled wells.	86	Figure 7.4. Maps of the three Special Study Areas showing the distribution of ammonium	120
Figure 6.7. Classification of survey sample sites by geological unit.	86	Figure 7.5. Maps of the three Special Study Areas showing the distribution of Fe.	121
Figure 6.8. Spatial distribution in calcium from the National Hydrochemical Survey.	88	Figure 7.6. Maps of the three Special Study Areas showing the distribution of Mn	121
Figure 6.9. Spatial variation of iron in groundwaters from the National Hydrochemical Survey.	89	Figure 7.7. Maps of the three Special Study Areas showing the distribution of dissolved organic carbon.	122
Figure 6.10. Spatial variation of manganese in groundwaters from the National Hydrochemical Survey.	89	Figure 7.8. Maps of the three Special Study Areas showing the distribution of sodium.	122
Figure 6.11. Combination distribution of arsenic and manganese in groundwaters from the National Hydrochemical Survey.	90	Figure 7.9. Maps of the three Special Study Areas showing the distribution of chloride.	122
Figure 6.12. Spatial variation of sodium in groundwaters from the National Hydrochemical Survey.	90	Figure 7.10. Maps of the three Special Study Areas showing the distribution of sulphate.	122
Figure 6.13. Spatial variation of potassium in groundwaters from the National Hydrochemical Survey.	91	Figure 7.11. Maps of the three Special Study Areas showing the distribution of bicarbonate.	123
Figure 6.14. Spatial variation of boron in groundwaters from the National Hydrochemical Survey.	91	Figure 7.12. Maps of the three Special Study Areas showing the distribution of total phosphorus.	123
Figure 6.15. Spatial variation of sulphate in groundwaters from the National Hydrochemical Survey.	92		

Figure 7.13. Maps of the three Special Study Areas showing the distribution of boron.	123	Figure 8.3. Part of the LGED upazila map of Lakshmipur showing the location of Mandari.	152
Figure 7.14. Maps of the three Special Study Areas showing the distribution of molybdenum.	124	Figure 8.4. Sketch map of Mandari prepared by the local DPHE staff.	152
Figure 7.15. Maps of the three Special Study Areas showing the distribution of uranium	124	Figure 8.5. SPOT image of Mandari village.	152
Figure 7.16. Cumulative frequency distributions of total arsenic in the Special Study Areas (aquifer depths not divided).	126	Figure 8.6. Part of the hand-drawn DLRS map of Mandari given to us by the Union Council Chairman.	153
Figure 7.17. Variation of total arsenic with depth.	127	Figure 8.7. A typical hand-pumped tubewell (HTW) in Mandari	153
Figure 7.18. Maps of the Special Study Areas showing the distribution of total arsenic	128	Figure 8.8. Walter Kosmus operating the Arsenator in the primary school at Amin Bazar.	154
Figure 7.19. Variation of total arsenic with redox potential (Eh) in groundwaters from the Special Study Areas.	129	Figure 8.9. Plot showing the comparison of arsenic analyses by the Arsenator (unfiltered sample, field analysis) and direct aspiration ICP-AES (filtered sample, BGS laboratory).	155
Figure 7.20. Maps of the three Special Study Areas showing the distribution of As(III)	129	Figure 8.10. Map showing the distribution of arsenic in Mandari well waters.	156
Figure 7.21. As(III)/AsT ratio against AsT concentration in each of the Special Study Areas.	130	Figure 8.11. Map showing a close-up view of the distribution of arsenic in SW Mandari well waters	157
Figure 7.22. Variation of total arsenic with total dissolved Fe concentration.	130	Figure 8.12. Map showing the distribution of iron in Mandari well waters.	157
Figure 7.23. Variation of total arsenic with total dissolved manganese concentration.	130	Figure 8.13. Plot of arsenic concentration versus iron concentration in Mandari well waters.	157
Figure 7.24. Variation of total arsenic with total phosphorus concentration.	131	Figure 8.14. Map showing the distribution of manganese in Mandari well waters.	158
Figure 7.25. Variation of total arsenic with alkalinity (HCO ₃) concentration.	131	Figure 8.15. Map showing the distribution of phosphorus in Mandari well waters.	158
Figure 7.26. Variation of total arsenic with molybdenum concentration.	132	Figure 8.16. Map showing the distribution of sulphate in Mandari wells waters.	159
Figure 7.27. Variation of total arsenic with sulphate concentration.	132	Figure 8.17. Map showing the distribution of sodium in Mandari well waters.	159
Figure 7.28. Variation of total arsenic with uranium concentration.	133	Figure 9.1. Different scales of variation and their relevance to different processes and objectives.	161
Figure 7.29. Variation of $\delta^{18}\text{O}$ with $\delta^2\text{H}$ in the groundwaters from the Special Study Areas.	133	Figure 9.2. Histograms of the arsenic and log arsenic data (n=3534).	163
Figure 7.30. Maps of the three Special Study Areas showing the distribution of $\delta^{18}\text{O}$	135	Figure 9.3. Variogram of the log As-data.	163
Figure 7.31. Maps of the three Special Study Areas showing the distribution of $\delta^2\text{H}$	135	Figure 9.4. Map of the district-mean arsenic concentrations (in $\mu\text{g L}^{-1}$) found in the DPHE/BGS National Hydrochemical survey.	164
Figure 7.32. Maps of the three Special Study Areas showing the distribution of $\delta^{13}\text{C}$	136	Figure 9.5. Histograms of the districts with a mean arsenic concentration of below $50 \mu\text{g L}^{-1}$ and those with a mean arsenic concentration of over $50 \mu\text{g L}^{-1}$.	165
Figure 7.33. Variation of $\delta^{13}\text{C}$ with alkalinity (HCO ₃) concentration.	136	Figure 9.6. Variograms of the districts with a mean arsenic concentration of below $50 \mu\text{g L}^{-1}$ and those with a mean arsenic concentration of over $50 \mu\text{g L}^{-1}$.	165
Figure 7.34. Variation of $\delta^{34}\text{S}$ as a function of sulphate concentration.	137	Figure 9.7. Behaviour of the Hermite-transformed variable for disjunctive kriging of arsenic concentrations	166
Figure 7.35. Chemical variation with depth in groundwater from piezometers, Chapai Nawabganj sampled on 1/12/99.	139	Figure 9.8. Comparison of estimated arsenic concentrations obtained by ordinary kriging and disjunctive kriging.	167
Figure 7.36. Chemical variation with depth in groundwater from piezometers, Faridpur sampled on 9/12/99.	139	Figure 9.9. Smoothed map showing the estimated arsenic concentrations in shallow wells (<150 m) based on disjunctive kriging.	168
Figure 7.37. Chemical variation with depth in groundwater from piezometers, Lakshmipur sampled on 20/11/99.	140	Figure 9.10. Probabilities, calculated using disjunctive kriging, that the arsenic-concentration exceeds specified thresholds.	169
Figure 8.1. Village life: inside one of the <i>paras</i> .	151		
Figure 8.2. Work in the fields.	151		

- Figure 9.11. Scatter diagrams of the calculated probabilities for the arsenic concentration to exceed a defined threshold against calculated arsenic concentration using disjunctive kriging. (a) Threshold = $5 \mu\text{g L}^{-1}$, (b) Threshold = $10 \mu\text{g L}^{-1}$, (c) Threshold = $50 \mu\text{g L}^{-1}$, (d) Threshold = $150 \mu\text{g L}^{-1}$. 170
- Figure 9.12. Number of people exposed to arsenic-concentrations above $50 \mu\text{g L}^{-1}$ using the calculated probabilities and the population density. 171
- Figure 9.13. Histogram of (a) normal and (b) log-transformed arsenic data from Lakshmipur. (c) shows the corresponding variogram. 171
- Figure 9.14. Histogram of (a) normal (b) log-transformed (b) data from Mandari. (c) shows the variogram for arsenic. 172
- Figure 10.1. Temporal variation in water level (metres below ground level) at the Chapai Nawabganj monitoring sites. 177
- Figure 10.2. Temporal variation in water level (metres below ground level) at the Faridpur monitoring sites. 177
- Figure 10.3. Temporal variation in water level (metres below ground level) measured at the Lakshmipur monitoring sites. 177
- Figure 10.4. Temporal variation in As at the Chapai Nawabganj monitoring sites. 178
- Figure 10.5. Temporal variation in As at the Faridpur monitoring sites. 179
- Figure 10.6. Temporal variation in As at the Lakshmipur monitoring sites. 179
- Figure 10.7. Temporal variation in Na at the Chapai Nawabganj monitoring sites. 180
- Figure 10.8. Temporal variation in Cl at the Chapai Nawabganj monitoring sites. 180
- Figure 10.9. Temporal variation in Na at the Faridpur monitoring sites. 181
- Figure 10.10. Temporal variation in Cl at the Faridpur monitoring sites. 181
- Figure 10.11. Temporal variation in Na at the Lakshmipur monitoring sites. 181
- Figure 10.12. Temporal variation in Cl at the Lakshmipur monitoring sites. 182
- Figure 10.13. Temporal variation in SO_4 at the Chapai Nawabganj monitoring sites. 182
- Figure 10.13. Temporal variation in SO_4 at the Chapai Nawabganj monitoring sites. 182
- Figure 10.14. Temporal variation in SO_4 at the Faridpur monitoring sites. 183
- Figure 10.15. Temporal variation in SO_4 at the Faridpur monitoring sites. 183
- Figure 10.16. Temporal variation in P at the Chapai Nawabganj monitoring sites. 184
- Figure 10.17. Temporal variation in phosphate-P at the Faridpur monitoring sites. 184
- Figure 10.18. Temporal variation in phosphate-P at the Lakshmipur monitoring site. 184
- Figure 11.1. Location of the various sediment samples studied. 187
- Figure 11.2. Scheme used for separation and analysis of sediment samples. 190
- Figure 11.2. Scheme used for separation and analysis of sediment samples. 190
- Figure 11.3. Photomicrographs of Faridpur sediment. 193
- Figure 11.4. SEM photomicrographs of polished thin sections from the DW1 (Rajarampur) and West Latifpur boreholes. 195
- Figure 11.5. SEM photomicrographs of sediments from the Faridpur piezometer borehole (FPW6). 196
- Figure 11.6. Examples of XRD traces of oriented $<2 \mu\text{m}$ fractions from the test boreholes in the Special Study Areas highlighting variations in the proportions of smectite, mica and chlorite. 197
- Figure 11.7. Variation of total As and Fe with depth for the three project boreholes. 202
- Figure 11.8. Relationship between total Fe and As in the 21 sediments from the three project exploration boreholes. 202
- Figure 11.9. Depth profiles of oxalate-extractable arsenic from the DW1 and DW2 boreholes in Chapai Nawabganj. 204
- Figure 11.10. Depth profiles of oxalate-extractable iron from the DW1 and DW2 boreholes in Chapai Nawabganj. 204
- Figure 11.11. Oxalate-extractable elements derived from core material from the DW1 (Rajarampur) DPHE/DU borehole. 205
- Figure 11.12. Oxalate-extractable elements derived from core material from the DW2 (Chanlai) DPHE/DU borehole. 206
- Figure 11.13. Depth profiles of oxalate-extractable arsenic from the three project boreholes. 207
- Figure 11.14. Depth profiles of oxalate-extractable iron from the three project boreholes. 207
- Figure 11.15. Depth profiles of oxalate-extractable phosphate-P from the three project boreholes. 207
- Figure 11.16. Depth profiles of oxalate-extractable potassium from the three project boreholes. 207
- Figure 11.17. Relationship between arsenic and iron extracted by acid ammonium oxalate from Bangladesh sediments and soils. 208
- Figure 11.18. Relationship between oxalate-extractable arsenic and iron for a range of sandy sediments from across Bangladesh. 209
- Figure 11.19. Relationship between arsenic extracted by acid ammonium oxalate and total arsenic determined by complete digestion of the sample followed by arsenic analysis by HG-AFS. 209
- Figure 12.1. Block diagram showing the basic geology and hydrogeology of the Bengal Basin. 214
- Figure 12.2. Block diagram showing the principal geochemical processes involved in the development of arsenic-contaminated groundwater in the Bengal Basin. 215

- Figure 12.3. Calculated percentage of arsenic(V) sorbed by hydrous ferric oxide from a $100 \mu\text{g As(V) L}^{-1}$ solution as a function of the amount of Fe as Hfo present. 220
- Figure 12.4. Calculated percentage of arsenic(III) sorbed by hydrous ferric oxide from a $100 \mu\text{g As(III) L}^{-1}$ solution as a function of the amount of Fe as Hfo present. 220
- Figure 12.5. Calculated sorption of As(V) by Hfo as a function of As(V) concentration and pH in 0.01M NaCl background electrolyte. 221
- Figure 12.6. Calculated sorption of As(III) by Hfo as a function of As(III) concentration and pH in 0.01M NaCl background electrolyte. 221
- Figure 12.7. Schematic diagram showing how the consequences of a high solid/solution ratio on pore water arsenic concentrations. 222
- Figure 12.8. Change in the calculated arsenic concentration in groundwater as a result of changes in the amount of As adsorbed to iron oxides. 226
- Figure 12.9. Five-layer model used to investigate vertical flushing of arsenic from a middle As-contaminated iron-rich layer of sediments 228
- Figure 12.10. Simulated flushing of arsenic-rich groundwater from an Fe-rich layer at 20–30 m depth. 229
- Figure 12.11. Simulated flushing of arsenic-rich groundwater from an Fe-rich layer at 20–30 m depth with very weak As(III) binding 229
- Figure 13.1. Effect of time on the reduction in total dissolved arsenic and As(III) following passive oxidation of three tubewell waters from Chapai Nawabganj. 239
- Figure 13.2. Comparison of As concentrations in a range of Bangladesh tubewell waters before and after a long period of standing. 240
- Figure 13.3. Map showing possible constraints on the future use of hand-pump tubewells (after NWMP, 2000). 251

List of Tables

Table 2.1. Major arsenic minerals occurring in nature	4	Table 4.10. Approximate wet season regional groundwater gradients (BWDB, 1993)	53
Table 2.2. Typical arsenic concentrations in common rock-forming minerals	5	Table 4.11. Summary of change in use of irrigation technologies, expressed as a percentage of the overall irrigation volume	56
Table 2.3. Typical arsenic concentrations in rocks, sediments, soils and other surficial deposits	6	Table 4.12. Summary of irrigation abstraction modes operating in Bangladesh during 1996-1997	56
Table 3.1. Average monthly discharge and sediment load of major rivers.	17	Table 4.13. Estimates of flow and time for flushing for the aquifer units of the Brahmaputra Channel between Faridpur and Dhamrai under present-day gradients	57
Table 3.2. Main stratigraphic units of the Cenozoic and Quaternary sediments within the Bengal Basin.	19	Table 4.14. Estimates of flow and time for flushing for the aquifer units of the Brahmaputra Channel between Faridpur and Dhamrai under early Holocene gradient	58
Table 3.3. Monsoon change during 0–30 ka BP related to sedimentation offshore of the Indus Fan (Von Rad et al., 1999)	23	Table 4.15. Estimates of flow rates and time for flushing for Upper Ganges, Lower Ganges and Mahananda Channel sequences at Chapai Nawabganj under present-day gradients	58
Table 3.4. Patterns of sediment deposition within Bengal deltaic environments during the Upper Pleistocene and Holocene	24	Table 4.16. Estimates of flow rates and time for flushing for a cross section through Faridpur (see Figure 4.9)	58
Table 3.5. Patterns of sediment deposition within Bengal fluvial environments during the Upper Pleistocene and Holocene	24	Table 4.17. Summary of aquifer parameters for the upper shallow, lower shallow and deep aquifers at Faridpur	59
Table 3.6. Radiocarbon dates of samples obtained from the Chapai Nawabganj test borehole (CPW5)	28	Table 5.1. Groundwater flow balance for Faridpur model from the Phase I report	65
Table 3.7. Lithology and facies of deposition recognised in the Faridpur test borehole (FPW6)	31	Table 5.2. Recharge estimate based on seasonal groundwater head fluctuations	65
Table 3.8. Radiocarbon dates of samples taken from the Faridpur test borehole (FPW6)	32	Table 5.3. Comparison of the layers referred to by different conceptual models used in this project	66
Table 3.9. Lithology and facies of deposition recognised in the Lakshmipur borehole log	32	Table 5.4. Sensitivity of calculated groundwater flows to various parameters	66
Table 3.10. Radiocarbon dates with depth of samples taken from the Lakshmipur test borehole (LPW6)	35	Table 5.5. Hydraulic conductivity values used in the various simulations	67
Table 3.11. A summary of the hydrogeological units of the Raipur-Lakshmipur-Eklashpur area	35	Table 5.6. Layering based on the lithological log of the Faridpur borehole and used in the VS4 simulation	67
Table 4.1. Percent of the population of Bangladesh with access to safe drinking water	47	Table 5.7. Effect of various representations of the lithological stratification on the steady state flow at various depths	68
Table 4.2. Main aquifer divisions within the fluvial and deltaic areas of Bangladesh	48	Table 5.8. Types of wells used and their abstraction	69
Table 4.3. The three-layer aquifer model	48	Table 5.9. Distribution of flow in the aquifer under natural and pumped conditions	70
Table 4.4. The four-layer aquifer model of Bangladesh (after EPC/MMP, 1991)	49	Table 5.10. Approximate times of travel from the water table in the well catchment area to the various targets with pumping	70
Table 4.5. Long term mean monthly rainfall and potential evapotranspiration for four cities in Bangladesh (Rashid, 1991)	49	Table 5.11. Distribution of flows by time of travel from the water table to the well screen	70
Table 4.6. Flooded areas 1954-1988	50	Table 6.1. Number of districts visited and wells sampled in each division	81
Table 4.7. The main aquifers in Bangladesh, their lithologies, relative ages and transmissivities (UNDP, 1982)	51	Table 6.2. Number of upazilas visited and wells sampled in each sampled district	81
Table 4.8. Relationship between average aquifer test results and geological formation	52		
Table 4.9. Correlation of lithology with hydraulic conductivity and specific yield (MMP/HTS, 1982; Davies and Herbert, 1990)	52		

Table 6.3. Percentage of wells in each division classified by well depth and division	82	Table 7.6. Percentage exceedances above the Bangladesh standard and the WHO guideline value for As in groundwaters (distinguished by aquifer) from the three study areas	127
Table 6.4. The number of wells sampled, classified by age and division	82	Table 7.7. Variations in groundwater quality with depth in a 262 m deep borehole in Lakshmipur (Kamarchat Bazar, 22°55.31'N 90°58.28'E)	127
Table 6.5. The percentage of wells sampled, classified by age and division	82	Table 7.8. Concentrations of dissolved gases in selected groundwater samples from the three study areas	134
Table 6.6. Distribution of arsenic concentrations in the complete dataset expressed as percentiles (n=3534)	83	Table 7.9. Summary of chemical compositions of groundwaters from the piezometers at Chapai Nawabganj, Faridpur and Lakshmipur, December 1999	138
Table 6.7. Percentage of samples below or exceeding various concentration thresholds (n=3534)	83	Table 7.10. Results of tritium analysis from piezometers and other nearby wells in the three study areas	141
Table 6.8. Number of administrative areas with at least one sampled well exceeding a drinking-water standard	84	Table 7.11. Radiocarbon and stable-isotope data for groundwater samples from the piezometers and from neighbouring tubewells	142
Table 6.9. Arsenic statistics for the twelve most contaminated districts	85	Table 7.12. Chemistry of pore water (in mg L ⁻¹) from DW1 (Rajarampur)	145
Table 6.10. Arsenic statistics for the twelve least-contaminated districts	85	Table 8.1. Distribution of sampled tubewells with depth in Mandari	155
Table 6.11. Two-way classification of tubewells according to their arsenic concentration and depth	85	Table 8.2. Distribution of sampled tubewells in Mandari classified by the year installed and depth	155
Table 6.12. Average concentration of arsenic in wells as a function of well depth	86	Table 8.3. Number of wells classified by both depth and arsenic concentration	156
Table 6.13. Classification of sample sites (n=3534) and average arsenic concentrations based on the estimated geological unit (sorted by decreasing average arsenic concentration)	87	Table 8.4. Classification of wells by depth and arsenic concentration, expressed as a percentage of the number of wells within a given depth interval	156
Table 6.14. Number of shallow wells (less than 150 m deep) in given arsenic and 'Year constructed' classes and exceeding water-quality standards	87	Table 9.1. Summary statistics for deep wells (>150 m) and shallow wells (<150 m)	162
Table 6.15. Percentage of shallow wells in given arsenic and 'Year constructed' classes	87	Table 9.2. District-wise analysis of variance (ANOVA) for the As measurements from the shallow wells	163
Table 6.16. Statistical summary and exceedances above WHO guideline values (GV) for groundwaters from the National Hydrochemical Survey analysed by ICP-MS	93	Table 9.3. Parameters used for ordinary and disjunctive kriging	166
Table 6.17. Chemical data for groundwaters from deep tubewells in Dhaka city	97	Table 9.4. Percentage of Bangladesh by area that exceeds a probability limit with respect to the 50 µg L ⁻¹ Bangladesh arsenic standard	170
Table 6.18. Summary results of the 1999 NESP six upazila survey	100	Table 9.5. Summary statistics for the Lakshmipur wells	171
Table 6.19. Extent of contamination of wells in the 1999 NESP survey of six upazilas	100	Table 9.6. Summary statistics for the deep wells (>150 m) and the shallow wells (<150 m) in Mandari	172
Table 6.20. Percentage of wells contaminated according to owner and well type	100	Table 10.1. Site details of monitored wells	176
Table 6.21. Results from four upazilas from the DPHE-UNICEF CBARP survey, and the NESP six-upazila survey,	101	Table 11.1. Source of sediment samples	188
Table 7.1. Analyses of representative groundwater samples from the three Special Study Areas	110	Table 11.2. Description of the twenty one samples used for detailed mineralogical and geochemical studies	189
Table 7.2. Summary statistics for field determinands and major elements in groundwaters from the three Special Study Areas	112	Table 11.3. Fractionation of the Chapai Nawabganj sediments from test borehole CPW5 by sieve, heavy mineral and magnetic separation	191
Table 7.3. Summary statistics for trace elements in groundwaters from the three Special Study Areas	114	Table 11.3. Fractionation of the Chapai Nawabganj sediments from test borehole CPW5 by sieve, heavy mineral and magnetic separation	191
Table 7.4. Summary statistics for trace elements in groundwaters from the three Special Study Areas	116	Table 11.4. Fractionation of the sediments from the Faridpur borehole FPW6 by sieve, heavy mineral and magnetic separation	192
Table 7.5. Summary statistics for trace-element and stable isotopic data in groundwaters from the three Special Study Areas	118	Table 11.5. Fractionation of the sediments from Lakshmipur borehole LPW6 by sieve, heavy mineral and magnetic separation	192

Table 11.6. Magnetic susceptibility (MS) measurements made on the subset of 21 samples from the three Special Study Areas	193	Table 11.13. Summary statistics for oxalate-extractable arsenic and iron from the sediments of the three project boreholes	206
Table 11.7. Summary of the clay minerals identified by X-ray diffraction	198	Table 11.14. Average oxalate-extractable constituents in sediments derived from sandy horizons from various sources across Bangladesh*	208
Table 11.8. Whole-rock geochemical data for the Chapai Nawabganj CPW5 samples	199	Table 11.15. Total organic carbon content of selected sediments	210
Table 11.9. Whole-rock geochemical data for the Faridpur FPW6 samples	200	Table 12.1. Geochemical processes that can cause an increase of the arsenic concentration in groundwaters	223
Table 11.10. Whole rock geochemical data for the Lakshmi-pur LPW6 samples	201	Table 12.2. Arsenic and major element chemistry of some Bangladesh rivers	224
Table 11.11. Arsenic concentrations in individual separated fractions of five selected samples	203	Table 13.1. Exceedances of various inorganic chemicals observed in the DPHE/BGS National Hydrochemical Survey*	233
Table 11.12. Chemical index of alteration (CIA) values for a range of minerals and rocks	203	Table 13.2. Temporal variations in chemical composition of three water samples from Chapai Nawabganj after standing in a container open to air for various times	239

Abbreviations

AAN	Asian Arsenic Network	IDA	International Development Association
BAMWSP	Bangladesh Arsenic Mitigation Water Supply Project	JICA	Japan International Cooperation Agency
BGS	British Geological Survey	LGED	Local Government Engineering Department, Government of the People's Republic of Bangladesh
BWDB	Bangladesh Water Development Board, Government of the People's Republic of Bangladesh	MMI	Mott MacDonald International
CEC	Centre of Environmental Chemistry, Hanoi National University	MML	Mott MacDonald Ltd
DANIDA	Danish Agency for Development Assistance	MMP	Sir M MacDonald and Partners
DCH	Dhaka Community Hospital	MPO	Master Plan Organisation
DFID	UK Department for International Development	NESP	National Emergency Screening Programme, part of BAMWSP
DPHE	Department of Public Health Engineering, Government of the People's Republic of Bangladesh	NERC	Natural Environment Research Council (UK)
DTW	Deep tubewell	NHS	DPHE/BGS National Hydrochemical Survey
DU	Dhaka University	NIPSOM	National Institute for Preventative & Social Medicine
DWASA	Dhaka Water Supply and Sewerage Authority	REE	Rare-earth element
EAWAG	Swiss Federal Institute for Environmental Science and Technology	SDDC	Silver diethyl dithiocarbamate
EGIS	Environment and Geographic Information System Supply Project for Water Sector Planning	SEM	Scanning electron microscopy
GBM	Ganges-Brahmaputra-Meghna	SOES	School of Environmental Studies, Jadavpur University, Calcutta
GoB	Government of the People's Republic of Bangladesh	SPARRSO	Space Research and Remote Sensing Organisation, Government of the People's Republic of Bangladesh
GPS	Global Positioning System	STW	Shallow tubewell
GSB	Geological Survey of Bangladesh	UNDP	United Nations Development Programme
HG-AFS	Hydride-generation atomic-fluorescence spectrometry	UNDTCD	United Nations Department for Technical Cooperation in Development
HTW	Hand-pump tubewell	UNICEF	United Nations Children's Emergency Fund
ICP-AES	Inductively-coupled-plasma atomic-emission spectrometry	USEPA	United States Environmental Protection Agency
ICP-MS	Inductively-coupled-plasma mass spectrometry	USGS	United States Geological Survey
		WHO	World Health Organisation
		XRF	X-ray fluorescence

Note: Use of the word 'upazila' in place of 'thana'

On April 20, 2000, the Government of Bangladesh issued a directive to use the word '*upazila*' in place of 'thana'. This reflects the passage of the Upazila Parishad Act (1998) which came into effect on February 1, 1999. The directive has been honoured in this report. '*Upazila*' is also sometimes spelt '*upazilla*'.